Coke Formation on Pt−Sn/Al₂O₃ Catalyst for Propane Dehydrogenation

Hai-Zhi Wang,[†] Li-Li Sun,[†] Zhi-Jun Sui,*[,†] Yi-An Zhu,[†] Guang-Hua Ye,[†] De Chen,[‡] Xing-Gui Zhou,[†] and Wei-Kang Yuan[†]

[†]State Key Laboratory of Chemical Engineering, East China University of Science and Technology, Shanghai 200237, China
[‡]Department of Chemical Engineering, Norwegian University of Science and Technology, N-7491 Trondheim, Norway

ⓢ *Supporting Information*

ABSTRACT: Catalyst deactivation by coking is one major problem for propane dehydrogenation (PDH). To develop catalysts with high resistance to coke, the analysis of coke becomes essential. In this work, an analysis procedure is proposed and validated to acquire the detailed locations and compositions of the coke formed on an as-synthesized Pt−Sn/Al₂O₃ catalyst. This procedure combines high-resolution transmission electron microscopy (HRTEM), FT-IR, Raman, thermogravimetric analysis (TG), and pyrolysis GC-MS; with this procedure, the systematic and quantitative analysis of coke can be achieved. The results show that the coke is located on the metal, in the vicinity of the metal, and on the support. Besides, aliphatics, aromatics, and pregraphite cokes are identified, and they account for 69.0, 4.4, and 26.6 wt %, respectively. Finally, an in situ DRIFT study is performed, and the results show that the aliphatic coke can be transformed into the aromatic coke and this transformation is related to the deep dehydrogenation reactions.

The coke formed on the Pt-Sn/Al₂O₃
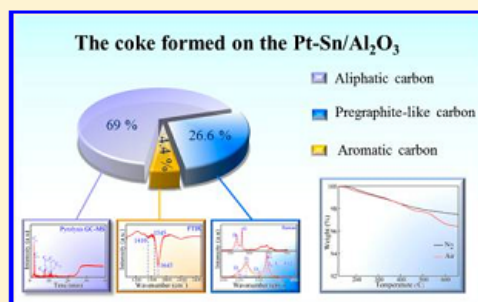
1. INTRODUCTION

Propene is one of the most important raw materials in the petrochemical industry, as it is the basic building block for a variety of commodity and specialty chemicals.[1] In recent years, the ever-growing demand for propene is hardly met by the traditional methods for producing propene, e.g., steam cracking and fluid catalytic cracking.[2] Hence, propane dehydrogenation (PDH) as a favorable alternative method for propene production grows in importance,[3] and it is estimated that over 14 million tons of propene will be produced from PDH annually by 2018 around the world.[4]

Pt based catalysts have been successfully used in some commercial PDH processes (e.g., UOP Oleflex and Uhde STAR), due to their superior activity in catalyzing PDH. However, these catalysts are prone to fast deactivation by coke formation under the high-temperature reaction condition, which becomes one of the major problems in existing PDH processes. For example, the Pt−Sn/ZnAl₂O₃ catalyst used in the Uhde STAR process can be deactivated by coking after only 7 h on steam.[4] Besides, the coked catalysts need to be frequently regenerated in a high-temperature oxidative atmosphere, which results in the sintering of Pt particles and subsequently irreversible catalyst deactivation.[5,6] Thus, it is of great significance to develop Pt based catalysts for PDH with high resistance to coke formation.[7,8] To achieve this, a fundamental understanding of the coke formation process on Pt based catalysts is required.

Coke formation on Pt based catalysts during PDH can be very complex, in which several active sites and many reactions are involved. On Pt sites, a series of hydrogenolysis, deep dehydrogenation, and polymerization reactions may lead to the coke deposition;[9,10] on acid sites of supports (e.g., Al₂O₃), skeletal isomerization, cracking, and polymerization may take part in the coking process.[3] Besides, the coke precursor formed on Pt sites can migrate to the acid sites with the addition of promoters.[6] The complex coking reactions on different active sites result in the complex locations and compositions of coke on Pt based catalysts for PDH. To better understand this coking process, it is essential to obtain the accurate locations and compositions of coke on the catalysts.

Some works have been devoted to analyzing the coke formed on Pt based catalysts for PDH. Larsson et al.[11] employed TPO to analyze the coke on a Pt−Sn/Al₂O₃ catalyst and found the coke is located on the metal, in the vicinity of the metal, and on the carrier; with the same Pt−Sn/Al₂O₃ catalyst, Larsson et al.[12] identified the reversible and irreversible coke on the catalysts using transient experiments. Then, Jackson et al.[13] used GC-MS to analyze the coke extracted from a Pt/Al₂O₃ catalyst, and they found a range of polyaromatics, among which pyrene and methyl pyrene are the

main components. They also deduced that C-1 fragments, rather than the C-3 units, are the primary source of these polyaromatics, based on the isotopic labeling experiments. Afterward, Vu et al.[6,14] employed XRD, XPS, and TPO to determine the composition of coke on PDH catalysts and concluded that the pregraphite-like carbon is the main component of coke on a Pt–Sn/Al$_2$O$_3$ catalyst. Weckhuysen and co-workers[15,16] introduced operando Raman in the study of the coking process on PDH catalysts, and they found the physicochemical properties of the coke on Pt/Al$_2$O$_3$ and Pt–Sn/Al$_2$O$_3$ catalysts change with time on stream and regeneration times. More recently, Redekop et al.[17] reported the coke on a Pt/Mg(Al)O$_x$ catalyst is comprised of graphene sheets by using high-resolution transmission electron microscopy (HRTEM). They also found the graphene sheets formed on small Pt particles (1.5−2 nm) would continuously shift onto the support and the graphene formed on large Pt particles (5−10 nm) does not shift onto the support but forms encapsulating graphitic layers. In our recent work, we used FT-IR and elemental analysis to characterize the coke on a Pt–Sn/Al$_2$O$_3$ catalyst and found the coke mainly contains aliphatic hydrocarbons.

Although the aforementioned works have provided some valuable knowledge about the coke formed on the Pt based catalysts for PDH, a comprehensive understanding of the locations and compositions of the coke is still lacking. Particularly, to the best of our knowledge, the quantitative analysis of the detailed coke composition has not been reported in the literature up to now. To conduct the comprehensive analysis of the coke formed on Pt based catalysts for PDH, an analysis procedure, which integrates various qualitative and quantitative characterization techniques, should be established and validated.

In this work, an analysis procedure was proposed to obtain the comprehensive information on coke formed on Pt–Sn/Al$_2$O$_3$, which integrated HRTEM, FT-IR, and Raman and introduced quantitative pyrolysis GC-MS (heating samples to high temperature (∼700 °C) within several milliseconds)[18−21] and thermogravimetric analysis (TG) using different carrier gases. The method was validated by comparing with the results of elemental analysis. By using this procedure, the detailed locations, compositions, and contents of the coke were qualitatively and quantitatively determined, and then, the possible coke formation mechanisms were deduced. At last, an in situ DRIFT study of the catalyst was conducted to probe the evolution of coke under elevated temperature. The results in this work are helpful for the rational design of Pt based catalysts for PDH with high resistance to coke, and the analysis procedure is also applicable for other reaction systems with coke deposition.

2. EXPERIMENTAL SECTION

2.1. Preparation of Catalyst. The catalyst support, γ-Al$_2$O$_3$, was prepared by calcining preudo-boehmite (Aldrich) at 600 °C for 8 h in air. The bimetallic Pt–Sn/Al$_2$O$_3$ was synthesized by the coimpregnation technique, in which H$_2$PtCl$_6$·6H$_2$O (99.9%, Sinopharm) and SnCl$_4$·5H$_2$O (99.9%, Sinopharm) were used as the Pt and Sn precursors, respectively. After the impregnation, the sample was dried at 120 °C overnight and then calcined in air at 500 °C for 4 h with a heating rate of 2 °C/min. The properties of the as-synthesized Pt–Sn/Al$_2$O$_3$ catalyst were collected in Table 1.

Table 1. Properties of the As-Synthesized Pt–Sn/Al$_2$O$_3$ Catalyst

S_{BET}[a] (m^2/g)	d_{pore}[a] (nm)	Pt dispersion[b] (%)	D_{CHEM}[b] (nm)	D_{TEM}[c] (nm)	Pt[d] (wt %)	Sn[d] (wt %)
182	6.1	80.2	1.4	1.3	1	1.8

[a]The BET surface area and volume-averaged pore diameter determined from the nitrogen adsorption−desorption isotherm, which is displayed in Figure S1. [b]Pt dispersion and average particle size of metal determined by CO chemisorption. [c]Average particle size of metal determined from HAADF-STEM, the representative images of which are given in Figure S2. [d]Pt and Sn contents determined by ICP-AES.

2.2. Catalyst Test. The PDH reaction was performed in a μBenchCAT reactor (Altamira Instrument, USA) at atmospheric pressure. The reactor was equipped with a quartz tube with an inner diameter of 6 mm and heated by an electrical furnace. Before the reaction, 100 mg of catalyst was loaded into the quartz tube and the catalyst was reduced in flowing hydrogen (10 mL/min) at 550 °C for 100 min. Then, the hydrogen was replaced by argon, and the temperature was raised to 575 °C with a heating rate of 10 °C/min. Afterward, the reaction mixture of propane, hydrogen, and argon (mole ratio 1:0.8:2.95) was fed into the reactor, and the total flow rate was 76 mL/min, yielding a weight hourly space velocity (WHSV) of propane of 14.7 h^{-1}. The effluent gas was analyzed with an online 4-channel microgas chromatograph (INFICON 3000, USA). The spent catalyst would be collected after the reactions and then prepared for characterization.

2.3. Catalyst and Coke Characterization. The Pt and Sn contents of the catalyst were determined by using a Varian 710-ES (Varian, China) inductively coupled plasma atomic emission spectrometer (ICP-AES). CO chemisorption was performed on an Autochem 2920 instrument (Micrometrics, USA), equipped with a thermal conductivity detector (TCD). Nitrogen adsorption−desorption isotherm measurements were conducted on an ASAP 2020 HD apparatus (Micromeritics, USA) at −196 °C, with all samples degassed at 350 °C under vacuum for 6 h. High-resolution transmission electron microscopy (HRTEM) images were taken using a JEM 2100 microscope (JEOL, Japan) operating at 200 kV. The high angle annular dark field scanning transmission electron microscopy (HAADF-STEM) images were taken on a Tecnai G2 F20 S-Twin microscope (FEI, USA) operated at 200 kV. The Fourier-transform infrared (FTIR) analysis was conducted on a NICOLET 6700 FTIR spectrometer (Thermo Fisher, USA) with a resolution of 4.0 cm^{-1} and the scanned wavenumber of 400−4000 cm^{-1}. Raman spectra were collected using an inVia Reflex Raman spectrometer (Renishaw, UK) equipped with a 514.5 nm Ar-ion laser beam and operated at room temperature. The thermogravimetric analysis (TG) was performed to determine the amount of coke, using a Pyris 1 instrument (PerkinElmer, USA) operated in nitrogen and air. The sample was dried at 100 °C for 2 h before the analysis, and then, the temperature was increased to 700 °C at a rate of 10 °C/min. The elemental analysis was conducted to obtain the atomic H/C ratio of coke, using a Vario EL III elemental analyzer (Elementar, Germany). The pyrolysis GC-MS analysis was performed to identify the coke composition, using an Agilent 7890A GC/5975C MSD system (Agilent Technologies, USA) equipped with a HP-5MS column (30 m × 0.25 mm, 0.25 μm film thickness). This method has been proved to be very

effective and convenient to determine the complex compositions of materials with high molecular weight, e.g., polymers, biomass, and cokes.[22,23] In the analysis, the sample was heated from 30 to 700 °C within several milliseconds, and then, the product was analyzed by GC-MS. The composition of coke was determined by matching the mass spectra collected in the National Institute of Standard and Technology (NIST) database (1998 version).

The diffuse reflectance infrared Fourier transform spectroscopy (DRIFT) study was carried out on a PerkinElmer Spectrum 100 FT-IR spectrometer (PerkinElmer, USA) equipped with a liquid nitrogen cooled mercury−cadmium−telluride (MCT) detector and an in situ Harrick Praying Mantis diffuse reflectance cell.[24] The DRIFT spectra were recorded with the temperature of 30−300 °C, a spectral resolution of 4 cm^{-1}, and an accumulation of 32 scans. The catalyst powder (~50 mg) was first reduced in flowing hydrogen (20 mL/min) at 200 °C for 0.5 h and subsequently cooled down to 30 °C in argon at the flow rate of 20 mL/min, followed by recording a background spectrum. Then, the sample was exposed to pure C$_3$H$_6$ (20 mL/min) at 30 °C for 0.5 h to ensure the steady-state conditions and subsequently purged with argon at the flow rate of 20 mL/min until no more gas-phase C$_3$H$_6$ was detected in the FT-IR spectrum, and then, this FT-IR spectrum was collected for analysis. After that, the sample was elevated to 100, 200, and 300 °C in argon at the flow rate of 20 mL/min, and then, the previous step was repeated to obtain the FT-IR spectra under the corresponding temperatures.

3. RESULTS AND DISCUSSION

3.1. Catalytic Performance.
The catalytic performance of the as-synthesized Pt−Sn/Al$_2$O$_3$ is displayed in Figure 1. The
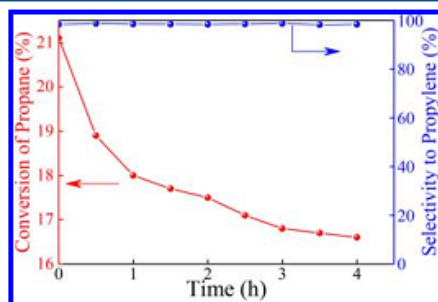

Figure 1. Propane conversion and propene selectivity of the as-synthesized Pt−Sn/Al$_2$O$_3$ at 575 °C.

selectivity to propene is 99%, and it only shows a negligible change with time on stream, while the conversion of propane decreases from 21.1% to 16.6% after reaction for 4 h. The decrease of conversion can be attributed to the catalyst deactivation by coke formation, as coke can cover active sites and subsequently reduce the available active sites for reaction. To obtain the detailed information on the coke formed during PDH, the spent catalyst is collected for analysis and these analysis results are displayed in the following sections.

3.2. Location of the Coke.
The derivative thermogravimetry (DTG) curves of the spent Pt−Sn/Al$_2$O$_3$ catalysts collected at 0.5, 2, and 4 h on stream are presented in Figure 2a. Two peaks are observed: the first weight loss peak in the temperature range of 400−500 °C can be attributed to the

weight loss of the coke located on the metal sites and in the vicinity of the metal sites; the second peak in the temperature range of 500−650 °C can be attributed to the weight loss of the coke on the support.[25] Besides, with the increase of reaction time, the first peak position shifts to higher temperature and its peak area increases, indicating that the coke located on and in the vicinity of the metal sites becomes more difficult to remove and the amount of this coke goes up. The shift of the first peak may be caused by the increased graphitization degree of the coke.[11] The area of the second peak increases with reaction time, indicating the continuous accumulation of the coke located on the support, which can be partially explained by the shift of coke precursor from metal sites to the support in the presence of tin. To further consolidate the role of tin in shifting coke, the coke formed on a Pt/Al$_2$O$_3$ catalyst was characterized, and these results are displayed in Figures S3 and S4. From Figures S3 and S4, we found that the coke on the Pt/Al$_2$O$_3$ catalyst is primarily located on the metal and in the vicinity of the metal, which indicates the coke on the metal would not be easily shifted onto the support without tin.

The representative HRTEM image of the spent Pt−Sn/Al$_2$O$_3$ catalysts collected at 4 h on stream is given in Figure 2b. The coke on the catalyst has a nonuniform morphology. The coke sheets are attached to the metal particles (label 1), located on the support (label 2), and lain on the metal surface (label 3), which is consistent with our DTG results. The fringe spacing of the coke ranges from 3.5 to 3.7 Å, which is larger than that of graphite (i.e., 3.35 Å).[26] Thus, this coke on the catalyst could be pregraphite carbon, which would be further confirmed by Raman analysis in the following subsection. These findings support that the catalyst deactivation is caused, at least partially, by the loss of active sites due to coke coverage during PDH.

3.3. Qualitative Analysis of the Coke Composition.
The FT-IR spectrum of the spent Pt−Sn/Al$_2$O$_3$ catalyst collected at 4 h on stream is presented in Figure 3. The adsorption bands between 1400 and 1450 cm^{-1} can be ascribed to the skeleton vibrations of branched aliphatics.[27] The bands between 1640 and 1680 cm^{-1} represent the stretching vibrations of C=C in alkenes,[28] and the bands between 1500 and 1630 cm^{-1} can be assigned to the vibrations of C=C in aromatics.[29] Apparently, the FT-IR spectrum indicates the coke on the spent catalyst contains aliphatics and aromatics. The peak area of aromatics is much smaller than that of aliphatics, implying the relatively lower amount of aromatics.

The Raman spectrum of the spent Pt−Sn/Al$_2$O$_3$ catalyst collected at 4 h on stream is displayed in Figure 4. Five peaks are identified in the spectrum, and they are located at 1336, 1602, 2700, 2920, and 3200 cm^{-1}, respectively. The peaks between 2700 and 3000 cm^{-1} can be attributed to the vibration of C−H bond in aliphatic hydrocarbons,[30,31] and the peak at 3200 cm^{-1} represents the vibration of C−H in aromatics.[32] Thus, the Raman spectrum indicates the presence of aliphatic and aromatic hydrocarbons in the coke, which is consistent with the observations of FT-IR.

The Raman peaks between 1200 and 1650 cm^{-1} are deconvoluted to analyze the detailed coke composition (see Figure 4b), as the Raman spectra of the carbonaceous materials (e.g., soot, graphene, graphite, and carbon nanofiber) show overlaps in that range.[33−35] After the deconvolution, four bands are obtained and they are labeled as G, D1, D3, and D4
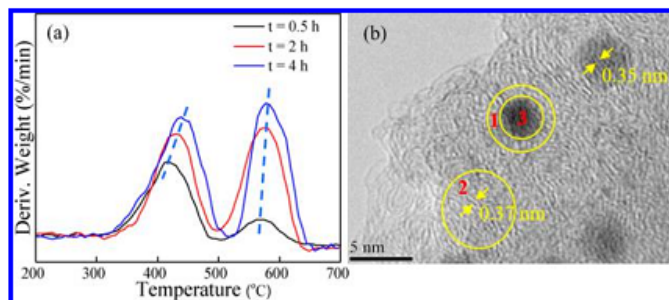
Figure 2. (a) DTG curves of the spent Pt−Sn/Al$_2$O$_3$ catalysts collected at different reaction times; (b) the representative HRTEM image of the spent catalyst collected at 4 h on stream.
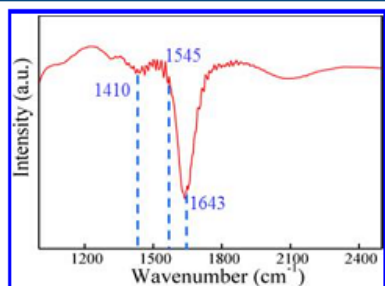

Figure 3. FT-IR curve of the spent Pt−Sn/Al$_2$O$_3$ catalyst collected at 4 h on stream.
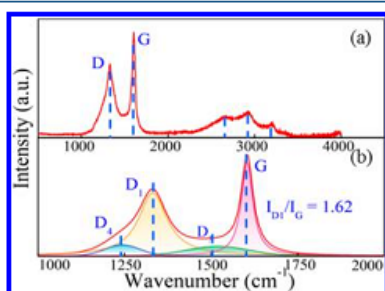

Figure 4. (a) Raman spectrum of the spent Pt−Sn/Al$_2$O$_3$ catalyst collected at 4 h on stream; (b) deconvolution of the peaks between 1200 and 1650 cm^{-1}.

according to the nomenclature proposed by Sadezky et al.[33] The G band at around 1580 cm^{-1} corresponds to an ideal graphitic lattice vibration mode with E$_{2g}$ symmetry;[36] the D$_1$ band at around 1350 cm^{-1} is called the defect band, which can be attributed to in-plane defects and heteroatoms.[16] The D$_3$ Raman band can be assigned to the amorphous carbon, and D$_4$ corresponds to the disordered graphitic lattice.[37] In Figure 4b, the G band is at 1602 cm^{-1} and higher than that of a perfect and large graphite crystal (i.e., 1575 cm^{-1}), indicating the coke could be graphite-like carbon species. This shift of G band to high wavenumber also implies that the crystal size of the graphite-like carbon could be small.[38,39] The ratio of I_{D1}/I_G is 1.62, suggesting the low graphitization degree of the coke.[40,41]

According to the above qualitative analysis using FT-IR and Raman, the coke formed on the Pt−Sn/Al$_2$O$_3$ catalyst can be divided into three types: aliphatics, aromatics, and pregraphite.

However, the quantities of the three types of coke cannot be determined by FT-IR and Raman, and the detailed compositions of aliphatics and aromatics have not been obtained. To acquire this quantitative information on the coke, TG and pyrolysis GC-MS analyses are introduced in this work and these results are provided in the following subsection.

3.4. Quantitative Analysis of the Coke Composition. TG curves of the spent Pt−Sn/Al$_2$O$_3$ catalyst are given in Figure 5. When the TG experiment is conducted in N$_2$
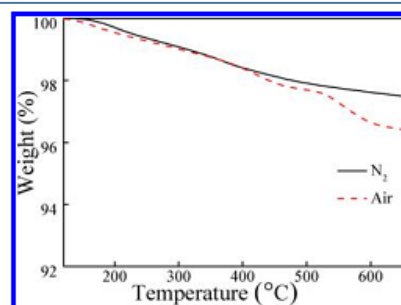

Figure 5. TG curves of the spent Pt−Sn/Al$_2$O$_3$ catalyst collected at 4 h on stream.

atmosphere, the weight loss is 2.86 wt % of the spent catalyst, which can be tentatively ascribed to the evaporation of volatile aliphatic and aromatic coke; when the TG experiment is performed in synthetic air, the weight loss is 3.90 wt %, which can be attributed to the burning of almost all the coke on the catalyst. The discrepancy in the coke amount is 1.04 wt %, which can be tentatively ascribed to the quantity of nonvolatile pregraphite in the coke.

The TG analysis gives the amount of pregraphite in the coke; however, the compositions and quantities of aliphatics and aromatics cannot be identified. To obtain this detailed information on the coke, pyrolysis GC-MS analysis was performed. Before analyzing these volatile components in the coke, a standard sample was tested by using pyrolysis GC-MS to validate this analytical method. The standard sample was prepared by mixing 13 typical paraffins and olefins with carbon number ranging from C8 to C28, which are listed in Table S2. The pyrolysis GC-MS result of the standard sample is shown in Figure 6b. The mass spectrum shows that the components are matched with those added in the standard sample and no other components are observed, indicating the degradation of the
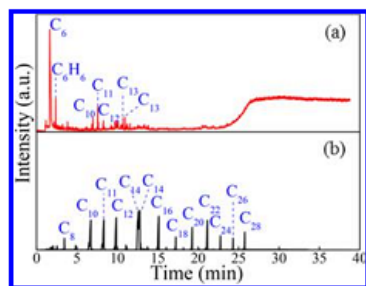
Figure 6. Pyrolysis GC-MS of (a) the spent Pt−Sn/Al$_2$O$_3$ catalyst collected at 4 h on stream; (b) the standard sample.

standard sample during the pyrolysis process is negligible. Besides, for the standard sample, the weight percentage of each component measured by pyrolysis GC-MS is close to the calculated one, as shown in Table S2. Thus, pyrolysis GC-MS is proven to be an accurate and efficient method to quantitatively determine the compositions of coke on the Pt−Sn/Al$_2$O$_3$ catalyst for PDH.

Then, pyrolysis GC-MS analysis was conducted to determine the detailed compositions of coke on the catalyst, and the results are displayed in Figure 6a and Table 2. The

Table 2. Dominant Components of Aliphatic and Aromatic Coke Formed on the Spent Pt−Sn/Al$_2$O$_3$ Catalyst Determined by Pyrolysis GC-MS

retain time (min)	compound name	weight percentage (%)
2.380	benzene	5.65
1.785	1-hexene	69.00
3.456	1-octene	2.15
6.704	n-decane	2.92
8.327	n-undecane	4.50
9.870	n-dodecane	2.46
11.118	1-tridecene	2.68
11.324	n-tridecane	2.85

results show that the coke contains aliphatics (primary components: C6−C13 alkanes and alkenes) and aromatics (primary component: benzene). It is generally believed that the aliphatics in coke are produced through polymerization and propene is the most possible monomer.[42] However, the carbon chain lengths of these detected aliphatics in this work are not all the multiples of three, suggesting that the degradation products of C3 species, i.e., C2 and C1 fragments, may also take part in the polymerization reactions for coke formation. Besides, aliphatics are the major components and account for around 94 wt % of the volatile coke (aliphatics and aromatics). When the TG analyses are combined in Figure 5, the aliphatics and aromatics account for 2.69 and 0.17 wt % of the spent catalyst. Thus, aliphatics, aromatics, and pregraphite account for 69.0, 4.4, and 26.6 wt % of the coke (see Table 2).

According to the compositions given in Table 2, the H/C molar ratio can be calculated using the following equations:

$$n = \sum_{i=1}^{p} G_i C_i \tag{1}$$

$$m = \sum_{i=1}^{p} S_i C_i \tag{2}$$

$$x = \sum_{i=1}^{q} T_i K_i \tag{3}$$

$$C = \frac{B}{12} + \frac{E}{M_1} \times n + \frac{D}{M_2} \times x \tag{4}$$

$$H = \frac{E}{M_1} \times m + \frac{D}{M_2} \times (2x - 6) \tag{5}$$

where G_i and S_i are the carbon number and hydrogen number of a specific aliphatic hydrocarbon i; C_i is the mole percentage of a specific aliphatic hydrocarbon i in the aliphatic coke; T_i and K_i denote the carbon number and the mole percentage of a specific aromatics i in the aromatic coke; M_1 and M_2 are the average molecular weights of aliphatics and aromatic cs; B, E, and D are the weight percentages of pregraphite, aliphatics, and aromatics, respectively. It should be noted that the hydrogen number of the pregraphitic is assumed to be zero in this calculation method, since pregraphitic is very deficient in hydrogen. The calculated H/C molar ratio for the coke on the spent Pt−Sn/Al$_2$O$_3$ catalyst is 1.56, as seen in Table 3. The H/

Table 3. Compositions of the Coke on Supported Pt−Sn Catalysts

samples	Pt−Sn/MgAl$_2$O$_4$[a]	Pt−Sn/Al$_2$O$_3$
total coke (wt % of the spent catalyst)	3.7	3.9
aliphatic coke (wt %)	65.7	69.0
aromatics coke (wt %)	15.4	4.4
pregraphitic coke (wt %)	18.9	26.6
calculated H/C molar ratio	1.48	1.56
H/C molar ratio from elemental analysis	1.41	1.55

[a]The characterization results of the spent Pt−Sn/MgAl$_2$O$_4$ catalyst collected at 4 h on stream are given in Figure S5.

C molar ratio is also determined by the elemental analyzer, and the value is 1.55, which is very close to the calculated one. To further consolidate the calculation method, the coke formed on a Pt−Sn/MgAl$_2$O$_4$[43] catalyst is quantitatively analyzed,[44−46] and the results are displayed in Figure S5 and summarized in Table 3. The H/C molar ratio of the coke on the Pt−Sn/ MgAl$_2$O$_4$ catalyst is close to the one determined from elemental analysis (see Table 3). These comparisons prove again that pyrolysis GC-MS is an accurate and facile method to quantitatively determine the coke compositions.

3.5. In Situ DRIFT Study. It is commonly believed that propene is critical for coke formation reactions,[47] since propene is very active in chemical properties. Here, in situ DRIFT study of propene on the Pt−Sn/Al$_2$O$_3$ catalyst was carried out to probe the mechanism of coke formation, and the results are given in Figure 7. At the temperature of 30 °C, an intense IR band at 1644 cm^{-1} is observed and can be assigned to the characteristic band of C=C stretching of propene;[48] the band at 2959 cm^{-1} is ascribed to C−H vibration in −CH$_3$ species.[49] When the temperature goes up to 100 °C, the intensity of the C=C stretching band significantly decreases and the band at 2959 cm^{-1} increases, indicating the formation of aliphatic coke. Further increasing the temperature to 200 °C, two bands at 1456 and 1565 cm^{-1}, which can be ascribed
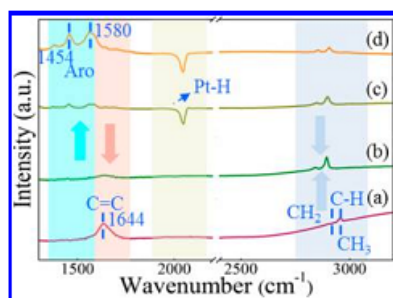
Figure 7. In situ DRIFT study of C_3H_6 on the Pt−Sn/Al$_2$O$_3$ catalyst at different temperatures: (a) 30 °C, (b) 100 °C, (c) 200 °C, and (d) 300 °C.

to the skeleton vibrations of aromatics ring,[50,51] are observed, but the intensity of the C−H vibration band decreases. Moreover, a derivative-shaped peak around 2000 cm^{-1}, which is caused by the surface Pt−H groups,[52] is found with the further depletion of the bands at 2029 and 2075 cm^{-1}. Thus, the quantity of aromatic coke increases with the elevated temperature, while the amount of aliphatic coke decreases with the elevated temperature. These results imply that the formation of aromatic coke could be associated with deep dehydrogenation reactions and the aliphatic coke may be transformed into the aromatic coke under elevated temperature.

4. CONCLUSIONS

In this work, a systematic analysis procedure, which combines HRTEM, FT-IR, Raman, TG, and pyrolysis GC-MS, is proposed and validated to obtain the qualitative and quantitative information on the coke formed on the Pt−Sn/Al$_2$O$_3$ catalyst for propane dehydrogenation. Through analyzing DTG curves and HRTEM images, it is found that the coke on the Pt−Sn/Al$_2$O$_3$ catalyst is located on the metal, in the vicinity of the metal, and on the support. From FT-IR and Raman spectra, three types of coke are identified and they are pregraphite, aromatics, and aliphatics. Integrating TG and pyrolysis GC-MS, the three types of coke on the Pt−Sn/Al$_2$O$_3$ catalyst are quantified. The aliphatics, aromatics, and pregraphite account for 69.0, 4.4, and 26.6 wt %, respectively. Besides, the carbon numbers of the aliphatics not only are the multiple of three, indicating the C1 and C2 species, but also may be the monomers for oligomerization reactions for coke formation. Finally, the in situ DRIFT study shows that the aliphatic coke can be transformed into aromatic coke under elevated temperature, and this transformation is associated with deep dehydrogenation reactions.

The results obtained in this work are helpful for the rational design of robust Pt based catalysts for PDH against deactivation by coke. The proposed analysis procedure of coke is facile and should be used to study other reaction systems with coke deposition.

■ ASSOCIATED CONTENT

ⓈSupporting Information

The Supporting Information is available free of charge on the ACS Publications website at DOI: 10.1021/acs.iecr.8b01313.

Preparation of the Pt/Al$_2$O$_3$ and Pt−Sn/MgAl$_2$O$_4$ catalysts; characterization of the as-synthesized Pt−Sn/

Al$_2$O$_3$ catalyst, the spent Pt/Al$_2$O$_3$ catalyst, and the Pt−Sn/MgAl$_2$O$_4$ catalyst; pyrolysis GC-MS analysis of the standard sample (PDF)

■ AUTHOR INFORMATION

Corresponding Author
*E-mail: zhjsui@ecust.edu.cn.
ORCID ●
Zhi-Jun Sui: 0000-0002-7819-6205
Yi-An Zhu: 0000-0001-6226-0711
Notes
The authors declare no competing financial interest.

■ REFERENCES

(1) Zhang, Y. W.; Zhou, Y. M.; Qiu, A. D.; Wang, Y.; Xu, Y.; Wu, P. C. Propane dehydrogenation on PtSn/ZSM-5 catalyst: Effect of tin as a promoter. *Catal. Commun.* **2006**, *7*, 860−866.

(2) Shan, Y. L.; Sui, Z. J.; Zhu, Y. A.; Chen, D.; Zhou, X. G. Effect of steam addition on the structure and activity of Pt−Sn catalysts in propane dehydrogenation. *Chem. Eng. J.* **2015**, *278*, 240−248.

(3) Lobera, M. P.; Téllez, C.; Herguido, J.; Menéndez, M. Transient kinetic modelling of propane dehydrogenation over a Pt−Sn−K/Al$_2$O$_3$ catalyst. *Appl. Catal., A* **2008**, *349*, 156−164.

(4) Sattler, J. J. H. B.; Ruiz-Martinez, J.; Santillan-Jimenez, E.; Weckhuysen, B. M. Catalytic Dehydrogenation of Light Alkanes on Metals and Metal Oxides. *Chem. Rev.* **2014**, *114*, 10613−10653.

(5) Van Sint Annaland, M.; Kuipers, J. A. M.; Van Swaaij, W. P. M. A kinetic rate expression for the time-dependent coke formation rate during propane dehydrogenation over a platinum alumina monolithic catalyst. *Catal. Today* **2001**, *66*, 427−436.

(6) Vu, B. K.; Song, M. B.; Ahn, I. Y.; Suh, Y. W.; Suh, D. J.; Kim, J. S.; Shin, E. W. Location and structure of coke generated over Pt−Sn/Al$_2$O$_3$ in propane dehydrogenation. *J. Ind. Eng. Chem.* **2011**, *17*, 71−76.

(7) Shi, L.; Deng, G. M.; Li, W. C.; Miao, S.; Wang, Q. N.; Zhang, W. P.; Lu, A. H. Al$_2$O$_3$ Nanosheets Rich in Pentacoordinate Al(3^+) Ions Stabilize Pt-Sn Clusters for Propane Dehydrogenation. *Angew. Chem., Int. Ed.* **2015**, *54*, 13994−13998.

(8) Xiong, H. F.; Lin, S.; Goetze, J.; Pletcher, P.; Guo, H.; Kovarik, L.; Artyushkova, K.; Weckhuysen, B. M.; Datye, A. K. Thermally Stable and Regenerable Platinum-Tin Clusters for Propane Dehydrogenation Prepared by Atom Trapping on Ceria. *Angew. Chem., Int. Ed.* **2017**, *56*, 8986−8991.

(9) Barias, O. A.; Holmen, A.; Blekkan, E. A. Propane Dehydrogenation over Supported Pt and Pt−Sn Catalysts: Catalyst Preparation, Characterization, and Activity Measurements. *J. Catal.* **1996**, *158*, 1−12.

(10) Bai, L. Y.; Zhou, Y. M.; Zhang, Y. W.; Liu, H.; Tang, M. H. Influence of Calcium Addition on Catalytic Properties of PtSn/ZSM-5 Catalyst for Propane Dehydrogenation. *Catal. Lett.* **2009**, *129*, 449−456.

(11) Larsson, M.; Hultén, M.; Blekkan, E. A.; Andersson, B. The Effect of Reaction Conditions and Time on Stream on the Coke Formed during Propane Dehydrogenation. *J. Catal.* **1996**, *164*, 44−53.

(12) Larsson, M.; Henriksson, N.; Andersson, B. Estimation of reversible and irreversible coke by transient experiments. *Stud. Surf. Sci. Catal.* **1997**, *111*, 673−680.

(13) Jackson, S. D.; Grenfell, J.; Matheson, I. M.; Munro, S.; Raval, R.; Webb, G. Deactivation and regeneration of alkane dehydrogenation catalysts. *Stud. Surf. Sci. Catal.* **1997**, *111*, 167−174.

(14) Vu, B. K.; Bok, S. M.; Ahn, I. Y.; Shin, E. W. Oxidation of Coke Formed Over Pt-Al$_2$O$_3$ and Pt-SBA-15 in Propane Dehydrogenation. *Catal. Lett.* **2009**, *133*, 376−381.

(15) Iglesias-Juez, A.; Beale, A. M.; Maaijen, K.; Weng, T. C.; Glatzel, P.; Weckhuysen, B. M. A combined in situ time-resolved UV−Vis, Raman and high-energy resolution X-ray absorption spectroscopy study on the deactivation behavior of Pt and PtSn propane dehydrogenation catalysts under industrial reaction conditions. *J. Catal.* **2010**, *276*, 268−279.

(16) Sattler, J. J.; Beale, A. M.; Weckhuysen, B. M. Operando Raman spectroscopy study on the deactivation of Pt/Al$_2$O$_3$ and Pt-Sn/Al$_2$O$_3$ propane dehydrogenation catalysts, *Phys. Phys. Chem. Chem. Phys.* **2013**, *15*, 12095−12103.

(17) Redekop, E. A.; Saerens, S.; Galvita, V. V.; González, I. P.; Sabbe, M.; Bliznuk, V.; Reyniers, M. F.; Marin, G. B. Early stages in the formation and burning of graphene on a Pt/Mg(Al)O x dehydrogenation catalyst: A temperature- and time-resolved study. *J. Catal.* **2016**, *344*, 482−495.

(18) Meier, D.; Faix, O. *Pyrolysis-Gas Chromatography-Mass Spectrometry* **1992**, 177−199.

(19) Zhang, B.; Zhong, Z. P.; Ding, K.; Song, Z. Production of aromatic hydrocarbons from catalytic co-pyrolysis of biomass and high density polyethylene: Analytical Py−GC/MS study. *Fuel* **2015**, *139*, 622−628.

(20) González-Pérez, J. A.; Almendros, G.; de la Rosa, J. M.; González-Vila, F. J. Appraisal of polycyclic aromatic hydrocarbons (PAHs) in environmental matrices by analytical pyrolysis (Py−GC/MS). *J. Anal. Appl. Pyrolysis* **2014**, *109*, 1−8.

(21) Nip, M.; Tegelaar, E. W.; Brinkhuis, H.; De Leeuw, J. W.; Schenck, P. A.; Holloway, P. J. Analysis of modern and fossil plant cuticles by Curie point Py-GC and Curie point Py-GC-MS: Recognition of a new, highly aliphatic and resistant biopolymer. *Org. Geochem.* **1986**, *10*, 769−778.

(22) Zhang, J.; Sui, Z. J.; Zhu, Y. A.; Chen, D.; Zhou, X. G.; Yuan, W. K. Composition of the Green Oil in Hydrogenation of Acetylene over a Commercial Pd-Ag/Al$_2$O$_3$ Catalyst. *Chem. Eng. Technol.* **2016**, *39*, 865−873.

(23) Matilainen, A.; Gjessing, E. T.; Lahtinen, T.; Hed, L.; Bhatnagar, A.; Sillanpää, M. An overview of the methods used in the characterisation of natural organic matter (NOM) in relation to drinking water treatment. *Chemosphere* **2011**, *83*, 1431−1442.

(24) Cao, Y. Q.; Sui, Z. J.; Zhu, Y. A.; Zhou, X. G.; Chen, D. Selective Hydrogenation of Acetylene over Pd-In/Al$_2$O$_3$ Catalyst: Promotional Effect of Indium and Composition-Dependent Performance. *ACS Catal.* **2017**, *7*, 7835−7846.

(25) Zhang, Y. W.; Zhou, Y. M.; Liu, H.; Wang, Y.; Xu, Y.; Wu, P. C. Effect of La addition on catalytic performance of PtSnNa/ZSM-5 catalyst for propane dehydrogenation. *Appl. Catal., A* **2007**, *333*, 202−210.

(26) Benedict, L. X.; Chopra, N. G.; Cohen, M. L.; Zettl, A.; Louie, S. G.; Crespi, V. H. Microscopic determination of the interlayer binding energy in graphite. *Chem. Phys. Lett.* **1998**, *286*, 490−496.

(27) Ibáñez, M.; Valle, B.; Bilbao, J.; Gayubo, A. G.; Castaño, P. Effect of operating conditions on the coke nature and HZSM-5 catalysts deactivation in the transformation of crude bio-oil into hydrocarbons. *Catal. Today* **2012**, *195*, 106−113.

(28) Cabrera, L. I.; Somoza, Á.; Marco, J. F.; Serna, C. J.; Morales, M. P. Synthesis and surface modification of uniform MFe2O4 (M = Fe, Mn, and Co) nanoparticles with tunable sizes and functionalities. *J. Nanopart. Res.* **2012**, *14*, 873.

(29) Ibarra, J. V.; Royo, C.; Monzón, A.; Santamaría, J. Fourier transform infrared spectroscopic study of coke deposits on a Cr$_2$O$_3$-Al$_2$O$_3$ catalyst. *Vib. Spectrosc.* **1995**, *9*, 191−196.

(30) Korhonen, S. T.; Airaksinen, S. M. K.; Bañares, M. A.; Krause, A. O. I. Isobutane dehydrogenation on zirconia-, alumina-, and zirconia/alumina-supported chromia catalysts. *Appl. Catal., A* **2007**, *333*, 30−41.

(31) Airaksinen, S. M. K.; Bañares, M. A.; Krause, A. O. I. In situ characterisation of carbon-containing species formed on chromia/alumina during propane dehydrogenation. *J. Catal.* **2005**, *230*, 507−513.

(32) Chua, Y. T.; Stair, P. C. An ultraviolet Raman spectroscopic study of coke formation in methanol to hydrocarbons conversion over zeolite H-MFI. *J. Catal.* **2003**, *213*, 39−46.

(33) Sadezky, A.; Muckenhuber, H.; Grothe, H.; Niessner, R.; Pöschl, U. Raman microspectroscopy of soot and related carbonaceous materials: Spectral analysis and structural information. *Carbon* **2005**, *43*, 1731−1742.

(34) Bernard, S.; Beyssac, O.; Benzerara, K.; Findling, N.; Tzvetkov, G.; Brown, G. E. XANES, Raman and XRD study of anthracene-based cokes and saccharose-based chars submitted to high-temperature pyrolysis. *Carbon* **2010**, *48*, 2506−2516.

(35) McGregor, J.; Huang, Z.; Parrott, E. P. J.; Zeitler, J. A.; Nguyen, K. L.; Rawson, J. M.; Carley, A.; Hansen, T. W.; Tessonnier, J. P.; Su, D. S.; Teschner, D.; Vass, E. M.; Knop-Gericke, A.; Schlögl, R.; Gladden, L. F. Active coke: Carbonaceous materials as catalysts for alkane dehydrogenation. *J. Catal.* **2010**, *269*, 329−339.

(36) Liu, J.; Zhao, Z.; Xu, C. M.; Duan, A. J.; Jiang, G. Y.; Gao, J. S.; Lin, W. Y.; Wachs, I. E. In-situ UV-Raman study on soot combustion over TiO$_2$ or ZrO$_2$-supported vanadium oxide catalysts. *Sci. China, Ser. B: Chem.* **2008**, *51*, 551−561.

(37) Han, Z. P.; Li, S. R.; Jiang, F.; Wang, T.; Ma, X. B.; Gong, J. L. Propane dehydrogenation over Pt-Cu bimetallic catalysts: the nature of coke deposition and the role of copper. *Nanoscale* **2014**, *6*, 10000−10008.

(38) Dresselhaus, M. S.; Dresselhaus, G.; Jorio, A.; Souza Filho, A. G.; Saito, R. Raman spectroscopy on isolated single wall carbon nanotubes. *Carbon* **2002**, *40*, 2043−2061.

(39) Tuinstra, F.; Koenig, J. L. Raman Spectrum of Graphite. *J. Chem. Phys.* **1970**, *53*, 1126−1130.

(40) Dumont, M.; Chollon, G.; Dourges, M. A.; Pailler, R.; Bourrat, X.; Naslain, R.; Bruneel, J. L.; Couzi, M. Chemical, microstructural and thermal analyses of a naphthalene-derived mesophase pitch. *Carbon* **2002**, *40*, 1475−1486.

(41) Li, J.; Naga, K.; Ohzawa, Y.; Nakajima, T.; Shames, A. I.; Panich, A. M. Effect of surface fluorination on the electrochemical behavior of petroleum cokes for lithium ion battery. *J. Fluorine Chem.* **2005**, *126*, 265−273.

(42) Li, Q.; Sui, Z.; Zhou, X.; Zhu, Y.; Zhou, J.; Chen, D. Coke Formation on Pt−Sn/Al$_2$O$_3$ Catalyst in Propane Dehydrogenation: Coke Characterization and Kinetic Study. *Top. Catal.* **2011**, *54*, 888−896.

(43) Shan, Y. L.; Wang, T.; Sui, Z. J.; Zhu, Y. A.; Zhou, X. G. Hierarchical MgAl$_2$O$_4$ supported Pt-Sn as a highly thermostable catalyst for propane dehydrogenation. *Catal. Commun.* **2016**, *84*, 85−88.

(44) Cremer, P. S.; Su, X. C.; Shen, Y. R.; Somorjai, G. A. Hydrogenation and Dehydrogenation of Propylene on Pt(111) Studied by Sum Frequency Generation from UHV to Atmospheric Pressure. *J. Phys. Chem.* **1996**, *100*, 16302−16309.

(45) Land, T. A.; Michely, T.; Behm, R. J.; Hemminger, J. C.; Comsa, G. STM investigation of single layer graphite structures produced on Pt(111) by hydrocarbon decomposition. *Surf. Sci.* **1992**, *264*, 261−270.

(46) Bocanegra, S. A.; Guerrero-Ruiz, A.; de Miguel, S. R.; Scelza, O. A. Performance of PtSn catalysts supported on MAl$_2$O$_4$ (M: Mg or Zn) in n-butane dehydrogenation: characterization of the metallic phase. *Appl. Catal., A* **2004**, *277*, 11−22.

(47) Jiang, F.; Zeng, L.; Li, S. R.; Liu, G.; Wang, S. P.; Gong, J. L. Propane Dehydrogenation over Pt/TiO$_2$−Al$_2$O$_3$ Catalysts. *ACS Catal.* **2015**, *5*, 438−447.

(48) Amakawa, K.; Wrabetz, S.; Krohnert, J.; Tzolova-Muller, G.; Schlogl, R.; Trunschke, A. In situ generation of active sites in olefin metathesis. *J. Am. Chem. Soc.* **2012**, *134*, 11462−11473.

(49) Shahid, G.; Sheppard, N. Infrared spectra and the structures of the chemisorbed species resulting from the adsorption of propene and propane on a Pt/SiO$_2$ catalyst. *Spectrochimica Acta A* **1990**, *46*, 999−1010.

(50) Meunier, F. C.; Zuzaniuk, V.; Breen, J. P.; Olsson, M.; Ross, J. R. H. Mechanistic differences in the selective reduction of NO by propene over cobalt- and silver-promoted alumina catalysts: kinetic and in situ DRIFTS study. *Catal. Today* **2000**, *59*, 287−304.

(51) Bodoardo, S.; Chiappetta, R.; Fajula, F.; Garrone, E. Ethene adsorption and reaction on some zeolites and pillared clays. *Microporous Mater.* **1995**, *3*, 613−622.

(52) Ko, M. K.; Frei, H. Millisecond FT-IR Spectroscopy of Surface Intermediates of C$_2$H$_4$ Hydrogenation over Pt/Al2O3 Catalyst under Reaction Conditions. *J. Phys. Chem. B* **2004**, *108*, 1805−1808.